International Journal of Mathematics and Statistics Studies

Vol.10, No.3, pp.49-81, 2022

Print ISSN: 2053-2229 (Print),

Online ISSN: 2053-2210 (Online)

Analysis of Unsteady Blood Flow Through a Stenosed Artery with Constant and Variable Viscosities

Jimoh, A
Department of Mathematical Sciences, Kogi State University, Anyigba. Nigeria.

Citation: Jimoh A. (2022) Analysis of Unsteady Blood Flow Through a Stenosed Artery with Constant and Variable Viscosities, *International Journal of Mathematics and Statistics Studies*, Vol.10, No.3, pp.49-81,

ABSTRACT: *This paper presents a theoretical study of the analysis of unsteady blood flow with constant and variable viscosities through a stenosed artery using a third grade fluid model. Incorporated into the models are the slip velocity and externally applied magnetic field. The methods employed in solving the equations governing the unsteady blood flow models with constant and variable viscosities are the Galerkin's weighted residual and Forth order Runge-Kutta. Important flow parameters such as flow velocity, flow rate, shear stress and flow resistance have been computed. Graphical representation shows that, for both cases of unsteady blood flow models with constant viscosity and variable viscosity, magnetic field and shear thinning increases with flow resistance but decreases the flow velocity, flow rate and shear stress. Increases in slip velocity and shear thinning lead to increases in flow velocity, flow rate and shear stress but decrease the flow resistance. Other parameters that can positively influence the flow velocity are the pressure gradient and Reynold number. Finally, the velocity profile of unsteady blood flow model with constant viscosity is higher than that with variable viscosity.*

KEYWORDS: Unsteady blood flow, Variable viscosity, constant viscosity, magnetic field, slip velocity, stenosed artery, third grade fluid model and Galerkin's Weighted residual methods.

INTRODUCITON

In a recent time, blood flow through normal or stenosed arteries has gained serious attention of many researchers [1-5] because blood and blood vessels are substantial health risk factors in the development of many cardiovascular diseases. Blood flow in the human circulatory system depends upon the pumping action of the heart. That is, the heart moves blood efficiently through the branching networks of arteries, capillaries and veins and the lungs cycle here quite effectively through the branching pulmonary passage thereby keeping the cells of our bodies alive and functioning.

It is well known fact that at high shear rates and large diameter arteries, blood, being predominantly a suspension of erythrocytes in plasma, behave as a Newtonian fluid. Some of the researchers that investigated the flow of blood through stenosed arteries and treating blood

as Newtonian fluid are (Amit and Shrivastar [6], Tanwar and Varshney [7], Ellahi *et al*,[8]). Existing literature in this area also reveals that shear rate of blood is low in ther stenosed region. A good many researchers (Hatami *et al* [9], Haleh *et al* [10], Aziz [11], Ikbal *et al* [12], Misra and Shit [13]) studied the non-Newtonian flow of blood from various perspectives.

In all the above investigations, only constant viscosity was considered. Variable viscosity of blood is another interesting area of study. The mathematical model of blood flow through a tapered artery with mild stenosis and variable viscosity was studied by Verma and Pariha [14]. Sanjeev and Chandraskhar [15] investigated hematocrit effect on the axisymmetric blood flow through stenosed arteries. Jimoh, *et al* [16] recently investigated hematocrit and slip velocity influence on third grade blood flow and heat transfer through a stenosed artery. They used weighted residual method to obtained the results in plotted graphs. The graphs reveals that, flow velocity and flow rate decreases while wall shear stress and resistance to flow increases when the hematocrit parameter increases.

The present study focused on the analysis of unsteady third grade blood flow with constant and variable viscosities through a stenosed artery. The externally applied magnetic field and slip velocity are also taken into consideration in this study.

MATHEMATICAL MODELS

The momentum equations describing the unsteady fluid flow models with constant viscosity and variable viscosity as obtained by Mohammed [17] and Jimoh [18] are respectively given as

$$\frac{\partial w}{\partial t} = \frac{\mu}{\rho r}\frac{\partial}{\partial r}\left(r\frac{\partial w}{\partial r}\right) + \frac{6\beta_3}{\rho}\left(\frac{\partial w}{\partial r}\right)^2\frac{\partial^2 w}{\partial r^2} + \frac{2\beta_3}{\rho r}\left(\frac{\partial w}{\partial r}\right)^2 + \frac{\alpha_1}{\rho r}\frac{\partial^2 w}{\partial r \partial t} + \frac{\alpha_1}{\rho}\frac{\partial^3 w}{\partial r^2 \partial t} - \frac{\partial \hat{P}}{\rho \partial z} - \frac{\sigma \beta_0^2}{\rho} w \qquad (2.1)$$

and

$$\frac{\partial w}{\partial t} = \frac{\mu_0}{\rho}\left[1 + N_1\left(1 - \left(\frac{r}{R_0}\right)^m\right)\right]\frac{1}{r}\frac{\partial}{\partial r}\left(r\frac{\partial w}{\partial r}\right) + \frac{6\beta_3}{\rho}\left(\frac{\partial w}{\partial r}\right)^2\left(\frac{\partial^2 w}{\partial r^2}\right) + \frac{2\beta_3}{r\rho}\left(\frac{\partial w}{\partial r}\right)^3 + \frac{\alpha_1}{r\rho}\frac{\partial^2 w}{\partial r \partial t}$$

$$+ \frac{\alpha_1}{\rho}\frac{\partial^3 w}{\partial r^2 \partial t} - \frac{1}{\rho}\frac{\partial \hat{P}}{\partial Z} - \sigma\frac{\beta_0^2 w}{\rho} \qquad (2.2)$$

As a result of the stenosed artery as shown in figure 1, the corresponding slip conditions to (2.1) and (2.2) are respectively given as

$$w = w_s \quad \text{at} \quad r = R(z) \qquad (2.3)$$

$$\frac{\partial w}{\partial r} = 0 \quad \text{at} \quad r = 0$$

and

$$\left.\begin{aligned} \text{w} = w_{N_1 s} \text{ at} \quad & r = R(z) \\ \frac{\partial w}{\partial r} = 0 \quad \text{at} \quad & r = 0 \end{aligned}\right\} \tag{2.4}$$

To non-dimensionalize equations (2.1) - (2.4), one introduces the following parameters and variables

$$\left.\begin{aligned} & \overline{w} = \frac{w}{d/t_0}, \qquad y = r/R_0 \\ & V_{01} = \frac{w_s t_0}{d}, \; V_{0N_1} = \frac{w_{N_1 s} t_0}{d} \end{aligned}\right\} \tag{2.5}$$

When equation (2.5) is substituted into (2.1) and (2.2), after simplifying one obtain respectively

$$\frac{\partial \overline{w}}{\partial \bar{t}} = \frac{1}{RE_1} \cdot \frac{\partial}{\partial y}\left(y \frac{\partial \overline{w}}{\partial y}\right) + \Omega\left(6\left(\frac{\partial \overline{w}}{\partial y}\right)^2 \frac{\partial^2 \overline{\omega}}{\partial y^2} + \frac{2}{y}\left(\frac{\partial \overline{w}}{\partial y}\right)^3\right) + \Omega_1\left(\frac{1}{y}\frac{\partial^2 \overline{w}}{\partial y \partial \bar{t}} + \frac{\partial^3 \overline{w}}{\partial y^2 \partial \bar{t}}\right) + G_1 - M_1 \overline{w} \tag{2.6}$$

and

$$\frac{\partial \overline{w}}{\partial \bar{t}} = \frac{1}{RE_{1N}}[1 + N_1(1 - y^m)].\frac{1}{y}\frac{\partial}{\partial y}\left(y \frac{\partial \bar{w}}{\partial y}\right) + \Omega_N\left(6\left(\frac{\partial \bar{w}}{\partial y}\right)^2 \left(\frac{\partial^2 \bar{w}}{\partial y^2}\right) + \frac{2}{y}\left(\frac{\partial \bar{w}}{\partial y}\right)^3\right)$$

$$+\Omega_{1N}\left(\frac{1}{y}\frac{\partial^2 \bar{w}}{\partial y \partial \bar{t}} + \frac{\partial^3 \bar{w}}{\partial y^2 \partial \bar{t}}\right) + G_{1N} - M_{1N}\bar{w} \tag{2.7}$$

as the dimensionless momentum equations describing the unsteady blood flow models with constant and variable viscosities.

The dimensionless slip conditions corresponding to (2.6) and (2.7) can be simplified respectively as

$$\left.\begin{aligned} \bar{w} &= V_{01} \quad \text{at} \quad y = \frac{R(z)}{R_0} = R_b \\ \frac{\partial \bar{w}}{\partial y} &= 0 \quad \text{at} \quad y = 0 \end{aligned}\right\} \tag{2.8}$$

A

$$\left.\begin{aligned} \bar{w} &= V_{0N_1} \quad \text{at} \quad y = R_b \\ \frac{\partial \bar{w}}{\partial y} &= 0 \quad \text{at} \quad y = \end{aligned}\right\} \tag{2.9}$$

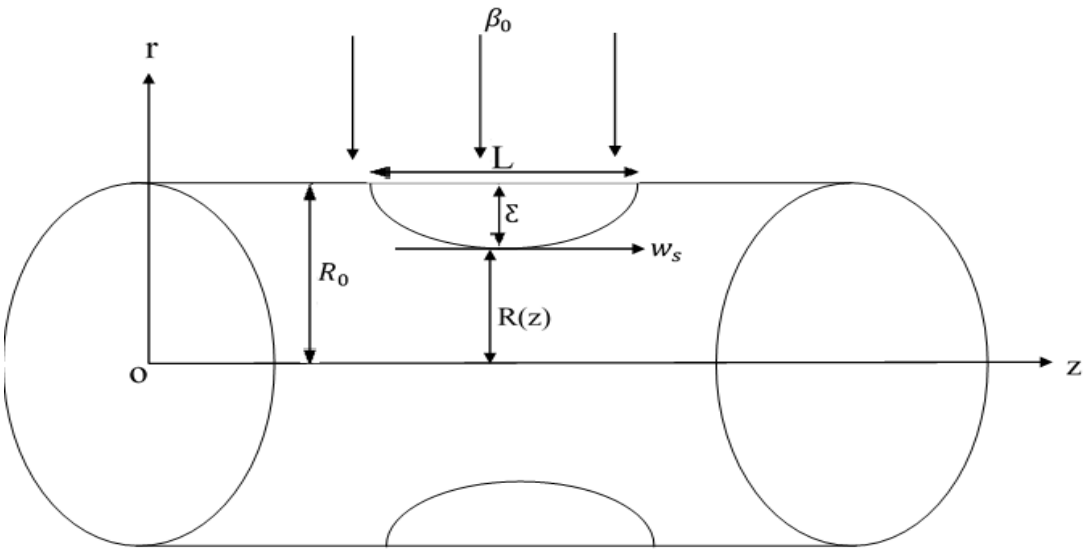

Figure1.Geometry of the stenosis

and has been described by Young [19] and Biswas [20]

$$\left.\begin{array}{ll} \frac{R(z)}{R_0} = 1 - \frac{\varepsilon}{2R_0}\left[1 + \frac{cos\pi z}{L}\right], & \text{for} \quad |z| \leq L \\ R_0, & \text{for} \quad |z| > L \end{array}\right\} \tag{2.9}$$

METHODS OF SOLUTION

In order to solve (2.6) using Galerkin weighted residual method, one assume a solution of the form

$$\bar{w}(y,t) = a_0(t) + a_1(t)y + a_2(t)y^2 \tag{3.1}$$

Subjecting (3.1) to the slip conditions (2.8) and after simplifying yields

$$\bar{w}(y,t) = \frac{V_{01}y^2}{Rb^2} + a_0(t)\left(1 - \frac{y^2}{Rb^2}\right) + a_2(t)\frac{y^2}{Rb^2}\left(1 - \frac{y^2}{Rb^2}\right) \tag{3.2}$$

Using $\bar{r} = \frac{y}{Rb}$ in (3.2) and after simplifying and dropping the bar one obtain

$$w(r,t) = V_{01}r^2 + a_0(t)(1 - r^2) + a_2(t)r^2(1 - r^2) \tag{3.3}$$

The residual for equation (2.6) can be written as

$$RR_1\big(r, a_0(t), a_2(t)\big) = \frac{\partial w}{\partial t} - G_1 - \frac{1}{RE_1}\frac{1}{r}\cdot\frac{\partial}{\partial r}\left(r\frac{\partial w}{\partial r}\right) - \Omega\left(6\left(\frac{\partial w}{\partial r}\right)^2\frac{\partial^2 w}{\partial r^2} + \frac{2}{r}\left(\frac{\partial w}{\partial r}\right)^3\right) -$$

$$\Omega_1\left(\frac{1}{r}\frac{\partial^2 w}{\partial r \partial t} + \frac{\partial^3 w}{\partial r^2 \partial t}\right) + M_1 w \tag{3.4}$$

substituting (3.3) into (3.4) and simplifying to obtain

$$RR_1\big(r, a_0(t), a_2(t)\big) = -G_1 - \frac{1}{RE_1}(4V_{01} + 4a_2(t) - 4a_0(t) - 16a_2(t)r^2) +$$

$$\dot{a}_0(t)(1 - r^2) + \dot{a}_2(t)r^2(1 - r^2) + 4\Omega_1\big(\dot{a}_0(t) - \dot{a}_2(t) + 4r^2\dot{a}_2(t)\big) - \Omega(48V_{01}^2r^2 -$$

$$144V_{01}^2a_0(t)r^2 + 144V_{01}^2a_2(t)r^2 - 480V_{01}^2a_2(t)r^4 + 144V_{01}a_0^2(t)r^2 -$$

$$40V_{01}a_0(t)a_2(t)r^2 + 960V_{01}a_0(t)a_2(t)r^4 + 144V_{01}a_2^2(t)r^2 -$$

$$144V_{01}a_2^2(t)r^4 4V_{01}a_2^2(t)r^6 + 144a_0^2a_2(t)r^2 - 480a_0^2(t)a_2(t)r^4 - 144a_0(t)a_2^2(t)r^2 +$$

$$960a_0(t)a_2^2(t)r^4 - 1344a_0(t)a_2^2(t)r^6 - 480a_2^3(t)r^4 + 1344a_2^3(t)r^6 - 48a_0^3(t)r^2 +$$

$$48a_2^3(t)r^2 - 1152a_2^3(t)r^8 - 128a_2^3(t)r^8 + 192V_{01}a_2^2(t)r^6 - 192a_0(t)a_2^2(t)r^6 +$$

$$192a_2^3(t)r^6 - 96V_{01}^2a_2(t)r^4 + 192V_{01}a_0(t)a_2(t)r^4 - 192V_{01}a_2^2(t)r^4 -$$

$$96a_0^2(t)a_2(t)r^4 + 192a_0(t)a_2^2(t)r^4 - 96a_2^3(t)r^4 + 16V_{01}^3r^2 - 48V_{01}^2a_0(t)r^2 +$$

$$48V_{01}a_0^2(t)r^2 - 96V_{01}a_0(t)a_2(t)r^2 + 48V_{01}a_2^2(t)r^2 - 16a_0^3(t) + 48a_0^2(t)a_2(t)r^2 -$$

$$48a_0(t)a_2^2(t)r^2 + 16a_2^3(t)r^2) - M_1(V_{01}r^2 + a_0(t) - a_0(t)r^2 + a_2(t)r^2 - a_2(t)r^4) \quad (3.5)$$

Differentiating (3.3) with respect to $a_0(t)\ and\ a_2(t)$, one obtain $(1-r^2)$ and $r^2(1-r^2)$ respectively as the weight functions.

Taking the orthogonality of the residue $RR_1(a_0(t), a_2(t), r)$ with respect to the weight functions $(1-r^2)$ and $r^2(1-r^2)$, one respectively obtain the following systems of nonlinear first order differential equations;

$$(1848 + 9240\Omega_1)\dot{a}_0(t) + (264 - 1848\Omega_1)\dot{a}_2(t) + 29568\Omega a_0^3(t) + 23600\Omega a_2^3(t) -$$

$$88704\Omega V_{01}a_0^2(t) - 191136\Omega V_{01}a_2^2(t) + 29568\Omega a_0(t)a_0^2(t) + 25344\Omega a_2(t)a_0^2(t) -$$

$$146784\Omega V_{01}a_0(t)a_0^2(t) - \left(1848M_1 + 354816\Omega V_{01}^2 - \frac{9240}{RE_1}\right)a_0(t) - \left(264M_1 -\right.$$

$$\left.25344\Omega V_{01}^2 - \frac{1848}{RE_1}\right)a_2(t) = 2310G_1 + \frac{9240V_{01}}{RE_1} + 22176\Omega V_{01}^2 + 462M_1V_{01} \quad (3.6)$$

and

$$(3432 + 24024\Omega_1)\dot{a}_0(t) + (1144 + 17160\Omega_1)\dot{a}_2(t) + 164736\Omega a_0^3(t) + 4872384\Omega a_2^3(t) - 494208\Omega V_{01} a_0^2(t) - 690768\Omega V_{01} a_0^2(t) - 6877728\Omega a_0^2(t)a_2(t) - 1677312\Omega a_2^2(t)a_0(t) - 1194336\Omega V_{01} a_0(t)a_2(t) - \left(3432M_1 - 1111968\Omega V_{01}^2 + \frac{24024}{RE_1}\right) a_0(t) - \left(429M_1 - 329472\Omega V_{01}^2 + \frac{17160}{RE_1}\right) a_2(t) = 6006G_1 + \frac{24024}{RE_1} + 123552\Omega V_{01}^2 + 2574M_1 V_{01} \quad (3.7)$$

By substituting the appropriate values of the parameters $G_1, V_{01}, RE_1, \Omega, \Omega_1, M_1$ and t into (3.6) and (3.7) and solve using forth order Runge-Kutta method, one obtain the values for $a_0(t)$ and $a_2(t)$ which when substituted into (3.3), the velocity profiles were obtained which are shown in table 1.

Similarly, to solve equation (2.7) following the same procedure as indicated above, one can write residue for (2.7) as

$$RR_2(a_0(t), a_2(t), r) = \frac{\partial w}{\partial t} - G_{1N} - \frac{1}{RE_{1N}}[1 + N_1(1 - r^m)].\frac{1}{r}\frac{\partial}{\partial r}\left(r\frac{\partial w}{\partial r}\right) - \Omega_N\left(6\left(\frac{\partial w}{\partial r}\right)^2\left(\frac{\partial^2 w}{\partial r^2}\right) - \frac{2}{r}\left(\frac{\partial w}{\partial r}\right)^3\right) - \Omega_{1N}\left(\frac{1}{r}\frac{\partial^2 w}{\partial r \partial t} + \frac{\partial^3 w}{\partial r^2 \partial t}\right) + M_{1N} w \quad (3.8)$$

Taking the shape of the profile $(m = 2)$ and substituting (3.3) into (3.8) and after simplifying in full to obtain.

$$RR_2(a_0(t), a_2(t), r) = -64\Omega_N r^2 V_{01N}^3 + M_{1N} r^2 V_{01N}^3 + 1280 a_2^3(t)\Omega_N r^8 - 1536 a_2^3(t)\Omega_N r^6 + 576 a_2^3(t)\Omega_N r^4 - M_{1N} a_2(t) r^4 + 64 a_0^3(t)\Omega_N r^2 - 64 a_2^3(t)\Omega_N r^2 -$$

$$M_{1N}a_0(t)r^2 + M_{1N}a_2(t)r^2 + 16\dot{a}_2(t)\Omega_{1N}r^2 + 4a_0(t) - 4a_2(t) + 16a_2(t)r^2 - 4V_{01N} - 1152a_0(t)a_2(t)\Omega_N r^4 V_{01N} + 384a_0(t)a_2(t)\Omega_N r^2 V_{01N} + 4\,N_1 r^2 V_{01N} - 16N_1 a_2(t)r^4 - \dot{a}_2(t)r^4 - 4N_1 a_0(t)r^2 + 20N_1 a_2(t)r^2 - \dot{a}_0(t)r^2 + \dot{a}_2(t)r^2 + M_{1N}a_0(t) + 4\dot{a}_0(t)\Omega_{1N} - 4\dot{a}_2(t)\Omega_{1N} - G_{1N} - 4N_1 V_{01N} + 4N_1 a_0(t) - 4Na_2(t) + \dot{a}_0(t) + 1536a_0(t)a_2^2(t)\Omega_N r^6 - 1536a_2^2(t)\Omega_N r^6 V_{01N} + 576a_0^2(t)a_2(t)\Omega_N r^4 - 1152a_0(t)a_2^2(t)\Omega_N r^4 + 1152a_2^2(t)\Omega_N r^4 V_{01N} + 576a_2(t)\Omega_N r^4 V_{01N}^2 - 192a_0^2(t)a_2(t)\Omega_N r^2 - 192a_0^2(t)\Omega_N r^2 V_{01N} + 192a_0(t)a_2^2(t)\Omega_N r^2 + 192a_0(t)\Omega_N r^2 V_{01N}^2 - 192a_2^2(t)\Omega_N r^2 V_{01N} - 192a_2(t)\Omega_N r^2 V_{01N}^2 \quad (3.9)$$

where **.** is the differentiation with respect to time t.

The following systems of nonlinear first order differential equations were obtained by following the same procedures as indicated earlier.

$$14784a_0^3(t)\Omega_N RE_{1N} + 12672a_0^2(t)a_2(t)\Omega_N RE_{1N} - 44352a_0^2(t)\Omega_N RE_{1N}V_{01N} + 14784a_0(t)a_2^2(t)\Omega_N RE_{1N} - 25344a_0(t)a_2(t)\Omega_N RE_{1N}V_{01N} + 44353a_0(t)\Omega_N RE_{1N}V_{01N}^2 + 2560a_2^3(t)\Omega_N RE_{1N} - 14784a_2^2(t)\Omega_N RE_{1N}V_{01N} + 12672a_2(t)\Omega_N RE_{1N}V_{01N}^2 - 14784\Omega_N RE_{1N}V_{01N}^3 + 924M_{1N}a_0(t)RE_{1N} + 132M_{1N}a_2(t)RE_{1N} + 231M_{1N}RE_{1N}V_{01N} + 4620\dot{a}_0(t)\Omega_{1N}RE_{1N} - 924\dot{a}_2(t)\Omega_{1N}RE_{1N} - 1155G_{1N}RE_{1N} + 3696N_1a_0(t) - 1584N_1a_2(t) - 3696N_1V_{01N} + 924\dot{a}_0(t)RE_{1N} + 132\dot{a}_2(t)RE_{1N} + 4620a_0(t) - 924a_2(t) - 4620V_{01N} = 0 \quad (3.10)$$

and

$$-82368a_0^3(t)\Omega_N RE_{1N} - 164736a_0^2(t)a_2(t)\Omega_N RE_{1N} + 257104a_0^2(t)\Omega_N RE_{1N}V_{01N} - 122304a_0(t)a_2^2(t)\Omega_N RE_{1N} + 329472a_0(t)a_2(t)\Omega_N RE_{1N}V_{01N} - 247104a_0(t)\Omega_N RE_{1N}V_{01N}^2 - 33792a_2^3(t)\Omega_N RE_{1N} + 122304a_2^2(t)\Omega_N RE_{1N}V_{01N} - 164736a_2(t)\Omega_N RE_{1N}V_{01N}^2 + 82368\Omega_N RE_{1N}V_{01N}^3 - 1716M_{1N}a_0(t)RE_{1N} - 572M_{1N}a_2(t)RE_{1N} - 1287M_{1N}RE_{1N}V_{01N} - 12012\dot{a}_0(t)\Omega_{1N}RE_{1N} - 8580\dot{a}_2(t)\Omega_{1N}RE_{1N} + 3003G_{1N}RE_{1N} - 6864N_1a_0(t) - 2288N_1a_2(t) + 6864N_1V_{01N} - 1716\dot{a}_0(t)RE_{1N} - 572\dot{a}_2(t)RE_{1N} - 12012a_0(t) - 8580a_2(t) + 12012V_{01N} = 0 \quad (3.11)$$

Substituting the appropriate values of the parameters Ω_N, RE_{1N}, M_{1N} Ω_{1N}, G_{1N}, V_{01N}, t and N_1 into (3.10) and (3.11) and solve using fourth order Runge-Kutta, one obtain the values for $a_0(t)$and $a_2(t)$ which when substituted into (3.3) and simplified, one obtain the velocity profiles $w(r,t)$ which are shown in table 2.

Volume Flow Rate

The volume flow rate denoted by Q can be simplified as

$$Q = 12\left[3V_{01}\left(R(z)\right)^4 + a_0(t)\left(6\left(R(z)\right)^2 - 3\left(R(z)\right)^4\right) + a_2(t)\left(3\left(R(z)\right)^4 - 2\left(R(z)\right)^6\right)\right] \quad (3.12)$$

Shear Stress

The shear stress denoted by τ_S can be simplified as

$$\tau_s = 2\mu R(Z)\left(V_{01} - a_0(t) + a_2(t) - 2R\left((Z)\right)^2 a_2(t)\right) + 16R(Z)\beta_3\left(V_{01} - a_0(t) + a_2(t) - 2\left(R(Z)\right)^2 a_2(t)\right) \quad (3.13)$$

Resistance to Flow

The resistance to flow can be denoted as ψ can be simplified as

$$\psi = \frac{-\frac{\partial \bar{P}}{\partial z}}{12\left[3V_{01}\left(R(z)\right)^4 + a_0(t)\left(6\left(R(z)\right)^2 - 3\left(R(z)\right)^4\right) + a_2(t)\left(3\left(R(z)\right)^4 - 2\left(R(z)\right)^6\right)\right]} \quad (3.14)$$

Table 1: Values of the Parameters Used in the Numerical Results and the corresponding Velocity Profile for the Unsteady Blood Flow Model with constant viscosity.

Figures	G_1	V_{01}	RE_1	Ω	Ω_1	M_1	t	w(r, t)
	1.5	0.25	0.9	10	1	0.35	0.5	$-0.1437r^2 + 0.3437 + 0.0335r^2(1-r^2)$
2a	2.0	0.25	0.9	10	1	0.35	0.5	$-0.1858r^2 + 0.3858 + 0.0296r^2(1-r^2)$
	2.5	0.25	0.9	10	1	0.35	0.5	$-0.2290r^2 + 0.4290 + 0.0262r^2(1-r^2)$
	1.5	0.25	0.9	10	1	0.35	0.5	$-0.2261r^2 + 0.4261 + 0.0260r^2(1-r^2)$
3a	1.5	0.25	0.9	10	1	0.65	0.5	$-0.2174r^2 + 0.4174 + 0.0249r^2(1-r^2)$
	1.5	0.25	0.9	10	1	0.95	0.5	$-0.2090r^2 + 0.4090 + 0.0237r^2(1-r^2)$
	1.5	0.25	0.9	10	1	0.35	0.5	$-0.0572r^2 + 0.2572 + 0.0009r^2(1-r^2)$
4a	1.5	0.35	0.9	10	1	0.35	0.5	$-0.1538r^2 + 0.3538 + 0.0019r^2(1-r^2)$
	1.5	0.45	0.9	10	1	0.35	0.5	$-0.2510r^2 + 0.4510 + 0.0030r^2(1-r^2)$
	1.5	0.25	0.9	10	1	0.35	0.5	$-0.3246r^2 + 0.5246 + 0.0499r^2(1-r^2)$
5a	1.5	0.25	0.9	20	1	0.35	0.5	$-0.3108r^2 + 0.5108 + 0.0538r^2(1-r^2)$
	1.5	0.25	0.9	30	1	0.35	0.5	$-0.2848r^2 + 0.4848 + 0.0554r^2(1-r^2)$

	1.5	0.25	0.9	10	1	0.35	0.5	$-0.1246r^2 + 0.3246 + 0.0168r^2(1-r^2)$
6a	1.5	0.25	0.9	10	5	0.35	0.5	$-0.2016r^2 + 0.4016 + 0.0073r^2(1-r^2)$
	1.5	0.25	0.9	10	9	0.35	0.5	$-0.2542r^2 + 0.4542 + 0.0001r^2(1-r^2)$
	1.5	0.25	0.3	10	1	0.35	0.5	$-0.0053r^2 + 0.2053 + 0.000Ir^2(1-r^2)$
7a	1.5	0.25	0.6	10	1	0.35	0.5	$-0.0094r^2 + 0.2094 + 0.0001r^2(1-r^2)$
	1.5	0.25	0.9	10	1	0.35	0.5	$-0.0091r^2 + 0.2091 + 0.0005r^2(1-r^2)$

Table 2: Values of the Parameters Used in the Numerical Results and the corresponding Velocity Profile for the Unsteady Blood Flow with Variable viscosity.

Figures	G_{1N}	V_{01N}	RE_{1N}	Ω_N	Ω_{1N}	M_{1N}	N_1	t	w(r, t)
	1.5	0.25	0.9	10	1	0.35	2	0.5	$0.2250 - 0.0250r^2 - 0.0119r^2(1-r^2)$
2b	2.0	0.25	0.9	10	1	0.35	2	0.5	$0.2588 - 0.0588r^2 - 0.0135r^2(1-r^2)$
	2.5	0.25	0.9	10	1	0.35	2	0.5	$0.2919 - 0.0919r^2 - 0.0138\ r^2(1-r^2)$
	1.5	0.25	0.9	10	1	0.35	2	0.5	$0.0218 - 0.0618r^2 - 0.0088r^2(1-r^2)$
3b	1.5	0.25	0.9	10	1	0.65	2	0.5	$0.0256 - 0.0540r^2 - 0.0086r^2(1-r^2)$
	1.5	0.25	0.9	10	1	0.95	2	0.5	$0.2503 - 0.0503r^2 - 0.0083r^2(1-r^2)$
	1.5	0.25	0.9	10	1	0.35	2	0.5	$0.3055 - 0.0555r^2 - 0.0111r^2(1-r^2)$
4b	1.5	0.35	0.9	10	1	0.35	2	0.5	$0.3954 - 0.0454r^2 - 0.0162r^2(1-r^2)$
	1.5	0.45	0.9	10	1	0.35	2	0.5	$0.4877 - 0.3773r^2 - 0.0206r^2(1-r^2)$
	1.5	0.25	0.9	10	1	0.35	2	0.5	$0.2974 - 0.0974r^2 - 0.0025r^2(1-r^2)$
5b	1.5	0.25	0.9	20	1	0.35	2	0.5	$0.2630 - 0.0630r^2 - 0.0082r^2(1-r^2)$

	1.5	0.25	0.9	30	1	0.35	2	0.5	$0.2582 - 0.0582r^2 - 0.0063r^2(1-r^2)$
	1.5	0.25	0.9	10	1	0.35	2	0.5	$0.2974 - 0.0974r^2 - 0.0025r^2(1-r^2)$
6b	1.5	0.25	0.9	10	5	0.35	2	0.5	$0.2872 - 0.0872r^2 - 0.0050r^2(1-r^2)$
	1.5	0.25	0.9	10	9	0.35	2	0.5	$0.2618 - 0.0618r^2 - 0.0088r^2(1-r^2)$
	1.5	0.25	0.3	10	1	0.35	2	0.5	$0.2381 - 0.0381r^2 - 0.0053r^2(1-r^2)$
7b	1.5	0.25	0.6	10	1	0.35	2	0.5	$0.2568 - 0.0568r^2 - 0.0067r^2(1-r^2)$
	1.5	0.25	0.9	10	1	0.35	2	0.5	$0.2618 - 0.0618r^2 - 0.0088r^2(1-r^2$

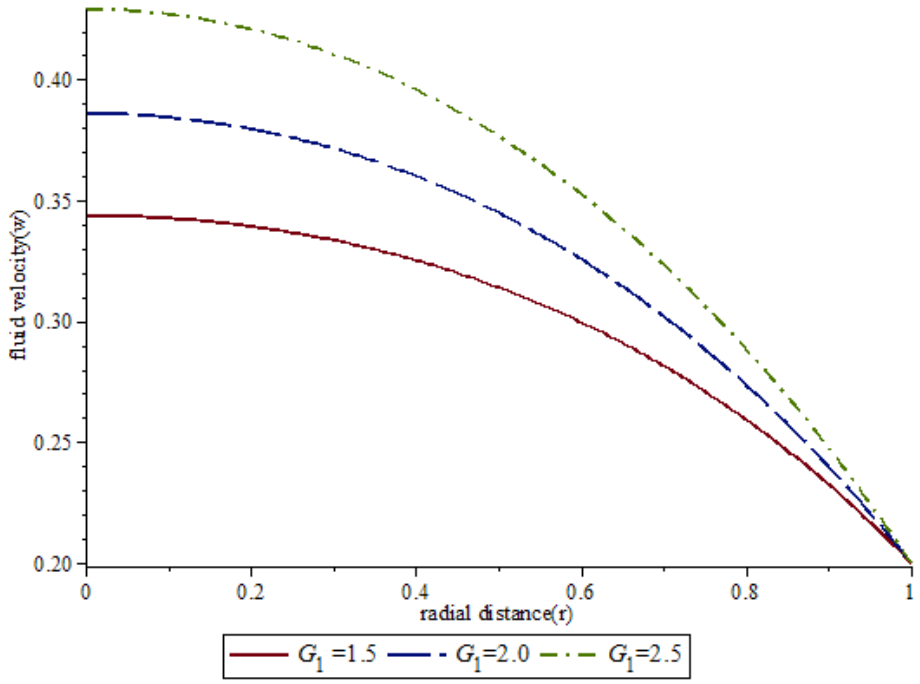

Figure 2a: Variation of Velocity Profile of the Unsteady Blood Flow Model with constant viscosity with increasing values of the Pressure Gradient in the radial direction.

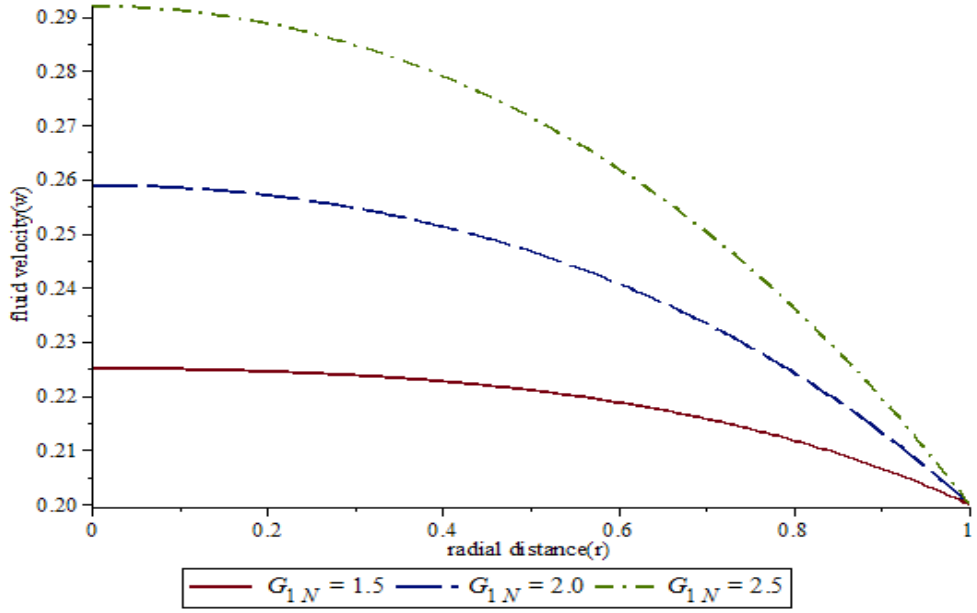

Figure 2b: Variation of Velocity Profile of the Unsteady Blood Flow Model with variable viscosity for various values of the Pressure Gradient in the radial direction.

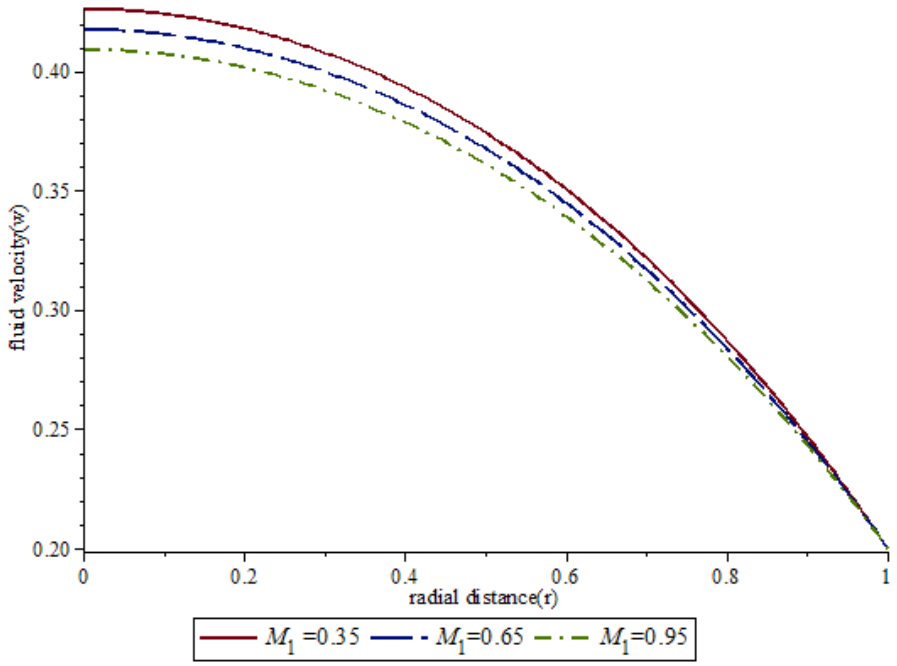

Figure 3a: Variation of Velocity Profile of the Unsteady Blood Flow Model with constant viscosity for various values of the Magnetic Field Parameter in the radial direction.

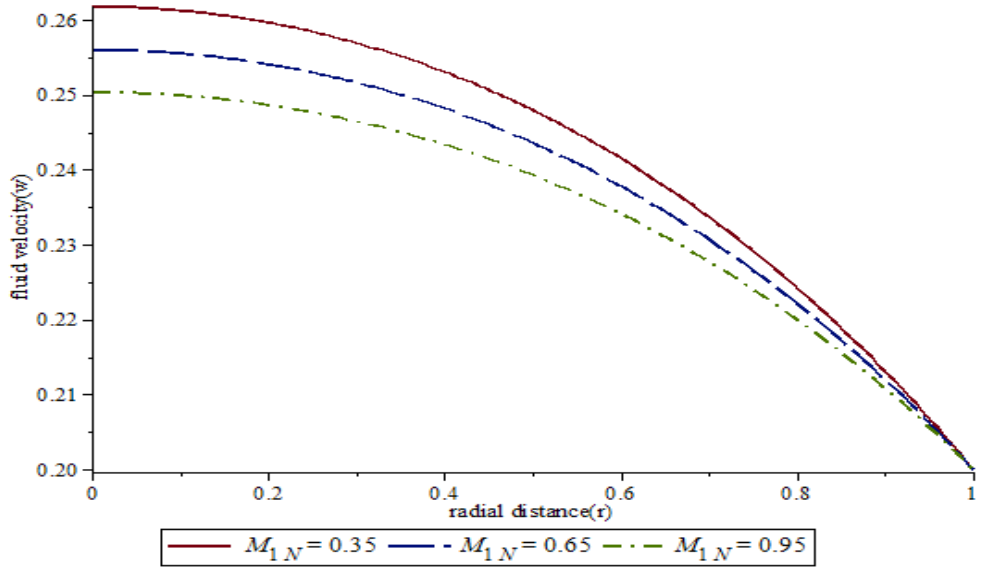

Figure 3b: Variation of Velocity Profile of the Unsteady Blood Flow Model with variable viscosity for various values of the Magnetic Field Parameter in the radial direction.

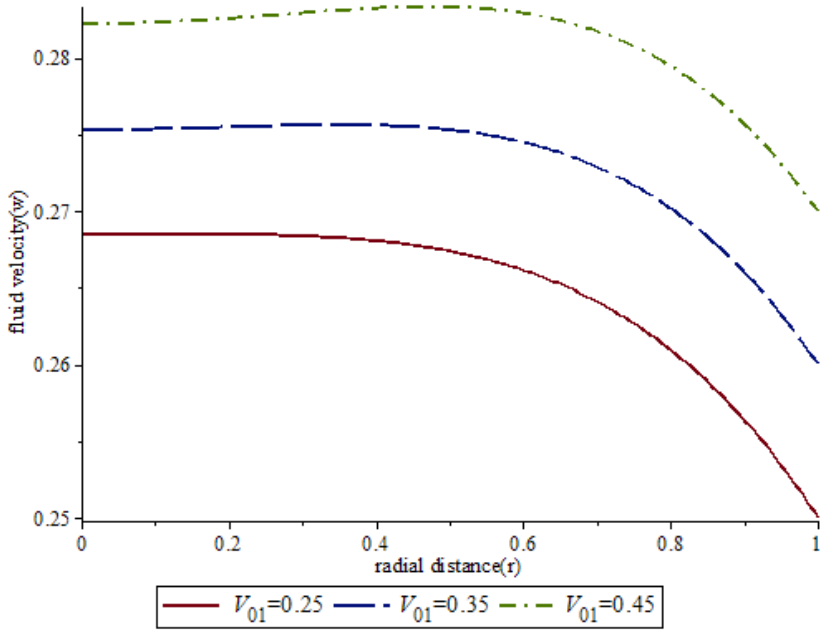

Figure 4a: Variation of Velocity Profile of the Unsteady Blood Flow Model with constant

viscosity for various values of the Slip Velocity in the radial direction.

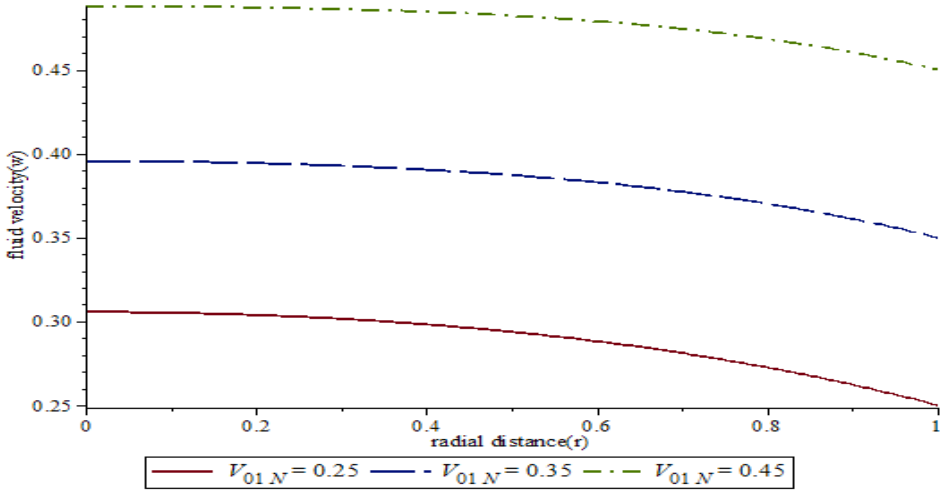

Figure 4b: Variation of Velocity Profile of the Unsteady Blood Flow Model with variable viscosity for various values of the Slip Velocity in the radial direction.

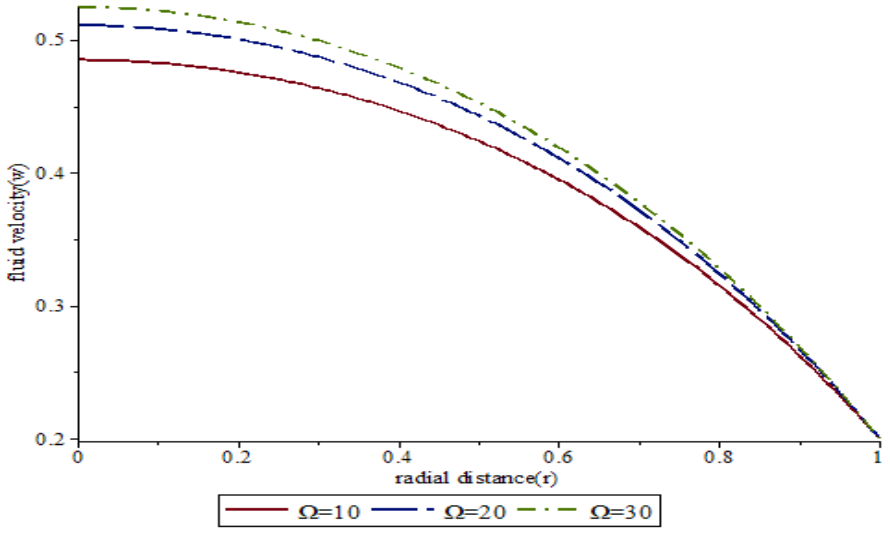

Figure 5a: Variation of Velocity Profile of the Unsteady Blood Flow Model with constant viscosity for various values of the Shear Thinning in the radial direction.

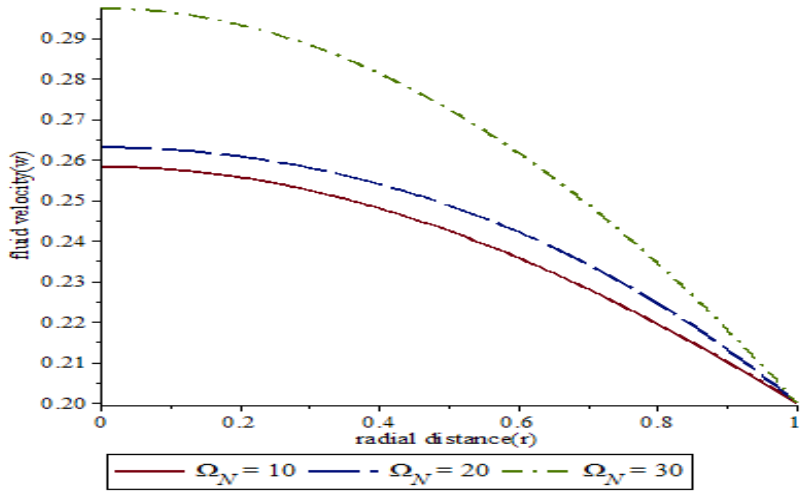

Figure 5b: Variation of Velocity Profile of the Unsteady Blood Flow Model with variable viscosity for various values of the Shear Thinning in the radial direction.

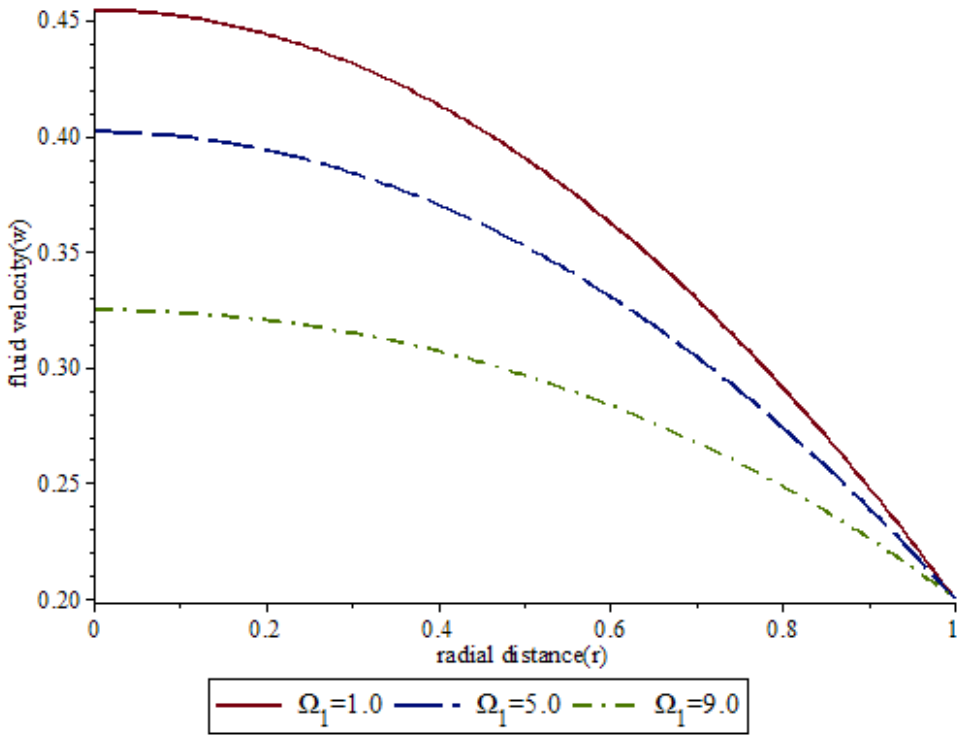

Figure 6a: Variation of Velocity Profile of the Unsteady Blood Flow Model with constant

Viscosity for various values of the Shear Thickening in the radial direction.

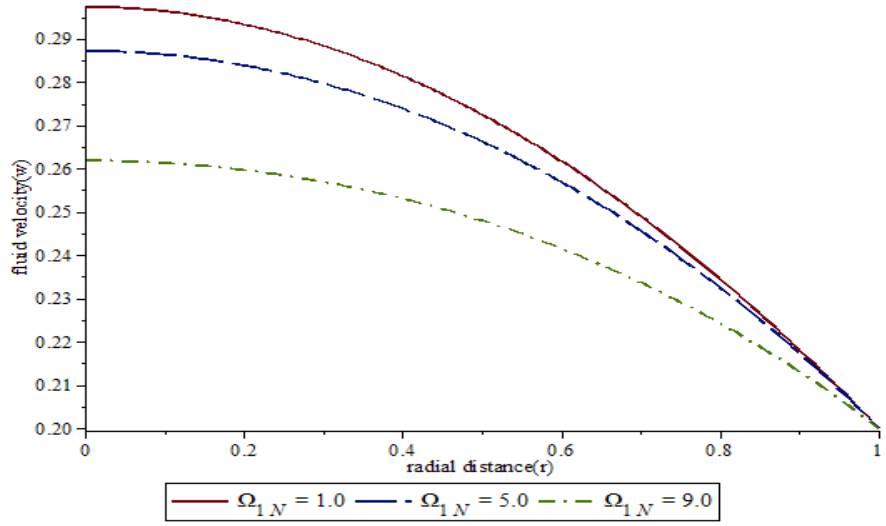

Figure 6b: Variation of Velocity Profile of the Unsteady Blood Flow Model with variable Viscosity for various values of the Shear Thickening in the radial direction.

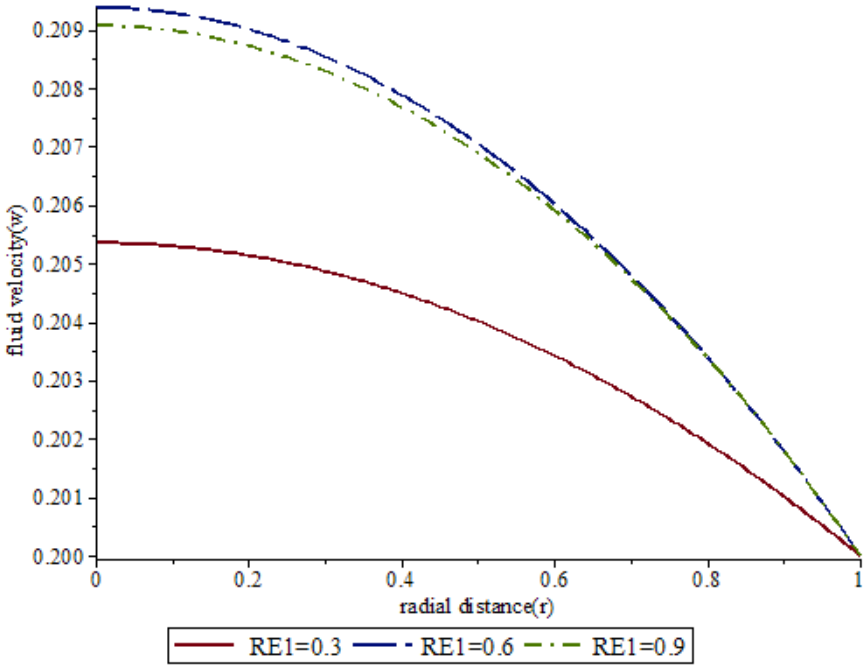

Figure 7a: Variation of Velocity Profile of the Unsteady Blood Flow Model with constant

Viscosity for various values of the Reynold number in the radial direction.

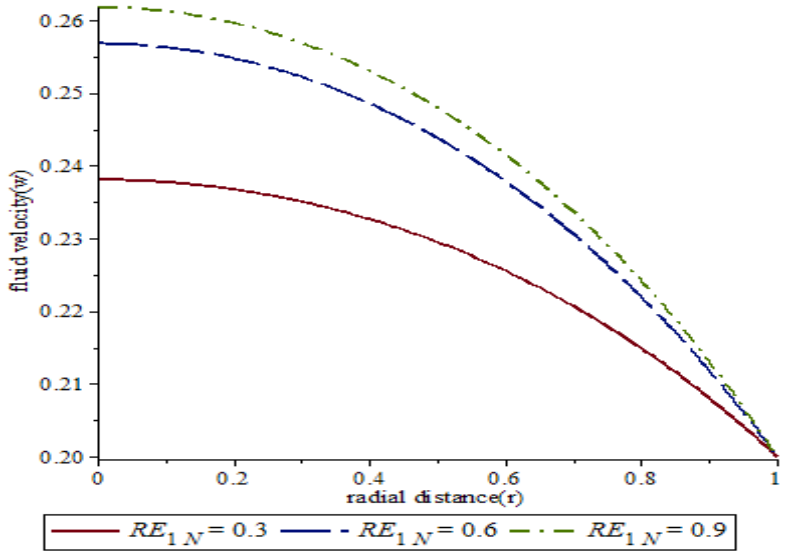

Figure 7b: Variation of Velocity Profile of the Unsteady Blood Flow Model with variable Viscosity for various values of the Reynold number in the radial direction.

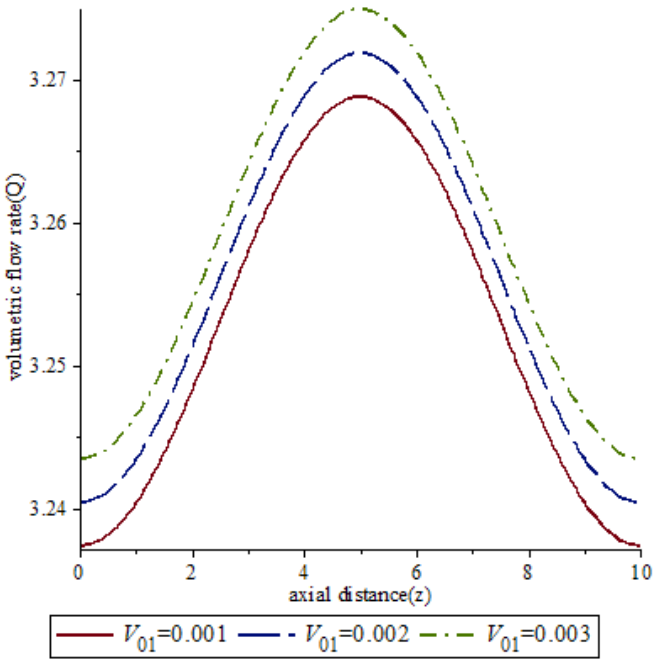

Figure 8a: Variation of Volume Flow Rate of Unsteady Blood Flow Model with constant

Viscosity for the various values of the Slip Velocity in the entire stenotic region along the axial direction.

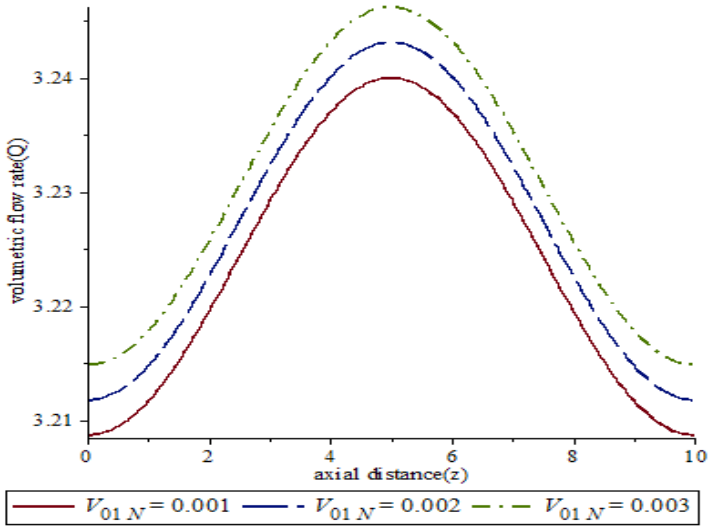

Figure 8b: Variation of Volume Flow Rate of Unsteady Blood Flow Model with variable Viscosity for the various values of the Slip Velocity in the entire stenotic region along the axial direction.

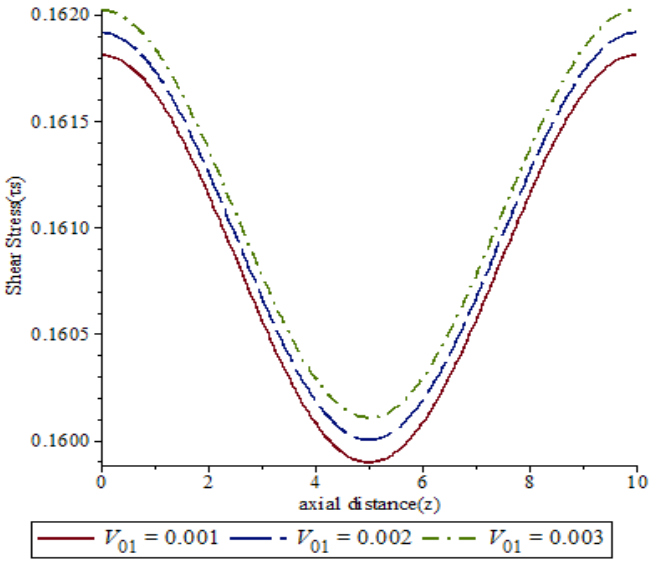

Figure 9a: Variation of Wall Shear Stress of Unsteady Blood Flow Model with constant

Viscosity for the various values of the Slip Velocity in the entire stenotic region along the axial direction.

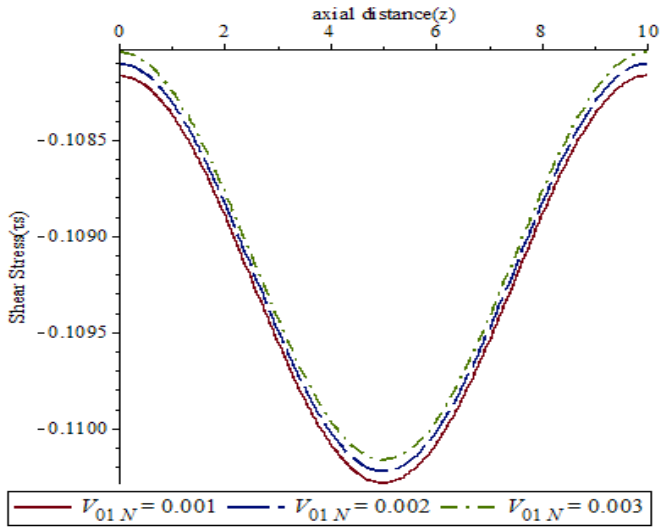

Figure 9b: Variation of Wall Shear Stress of Unsteady Blood Flow Model with variable Viscosity for the various values of the Slip Velocity in the entire stenotic region along the axial direction.

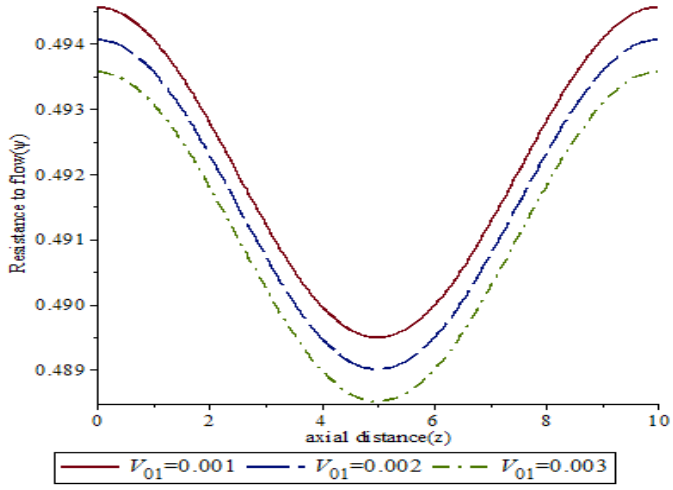

Figure 10a: Variation of Wall Shear Stress of Unsteady Blood Flow Model with constant Viscosity for various values of the Slip Velocity in the entire stenotic region along the axial direction.

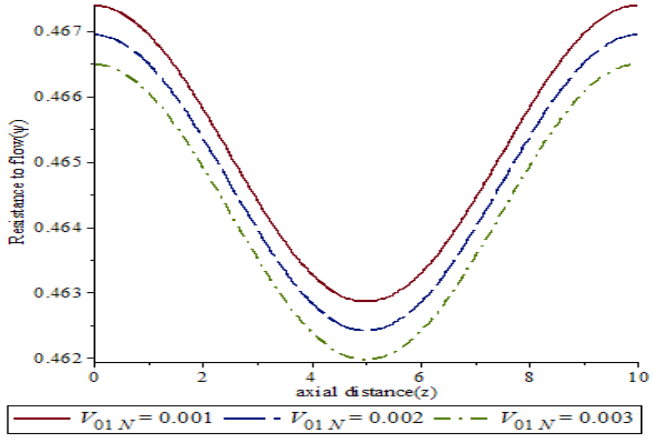

Figure 10b: Variation of Wall Shear Stress of Unsteady Blood Flow Model with variable Viscosity for various values of the Slip Velocity in the entire stenotic region along the axial direction.

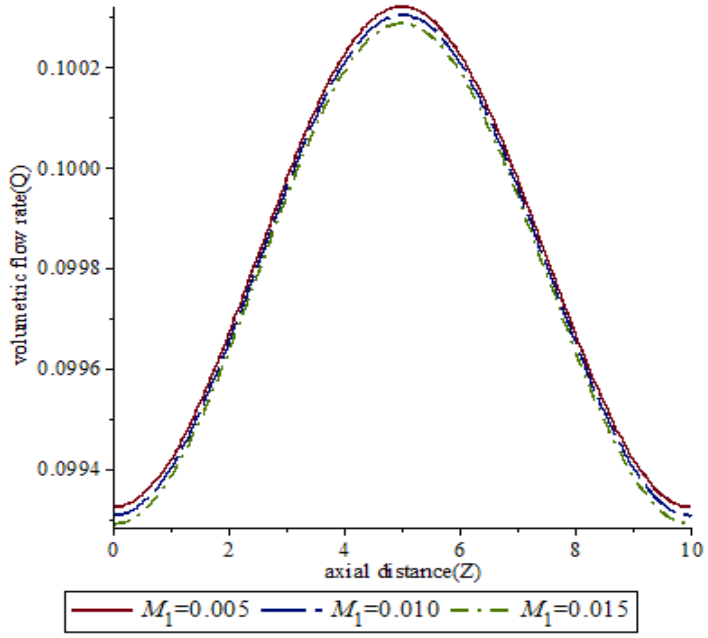

Figure 11a: Variation of Volume Flow Rate of Unsteady Blood Flow Model with constant viscosity for various values of the Magnetic Field Parameter in the entire stenotic region along the axial direction.

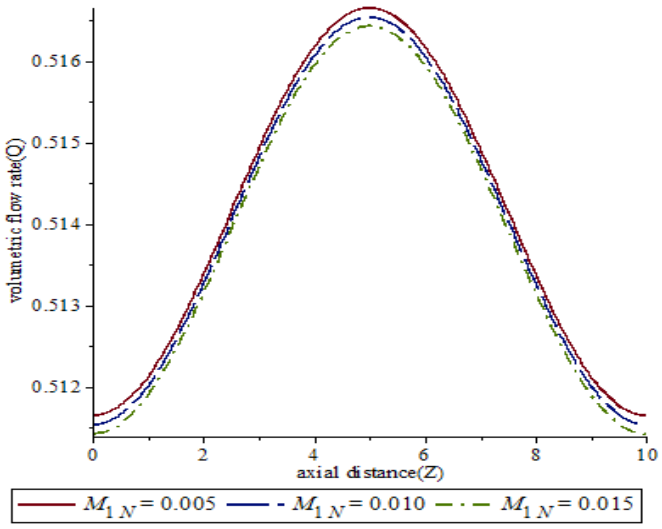

Figure 11a: Variation of Volume Flow Rate of Unsteady Blood Flow Model with constant viscosity for various values of the Magnetic Field Parameter in the entire stenotic region along the axial direction.

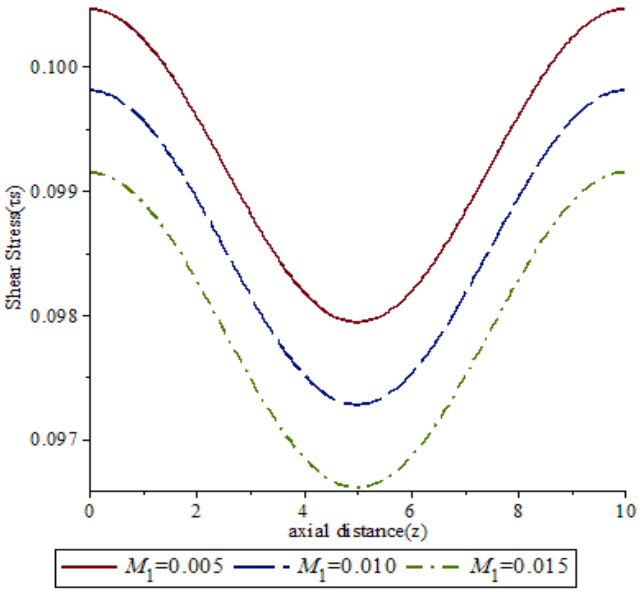

Figure 12a: Variation of Wall Shear Stress of Unsteady Blood Flow Model with constant viscosity for various values of the Magnetic Field Parameter in the entire stenotic region along the axial direction.

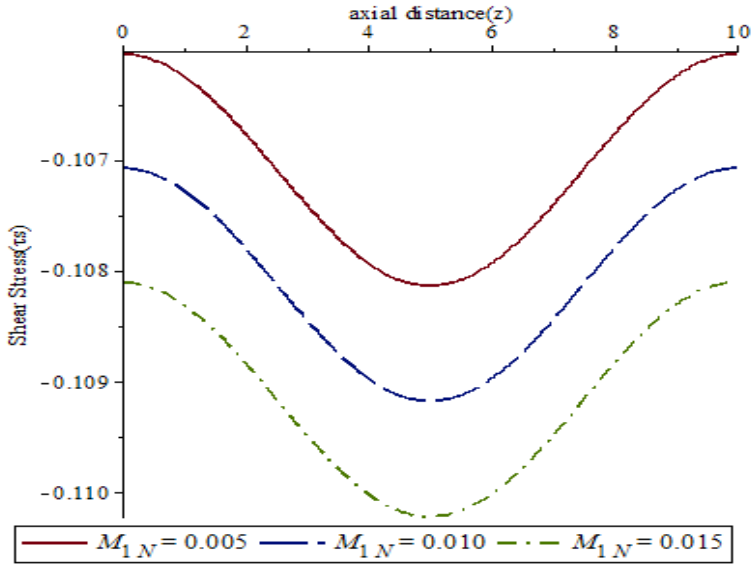

Figure 12b: Variation of Wall Shear Stress of Unsteady Blood Flow Model with variable viscosity for various values of the Magnetic Field Parameter in the entire stenotic region along the axial direction.

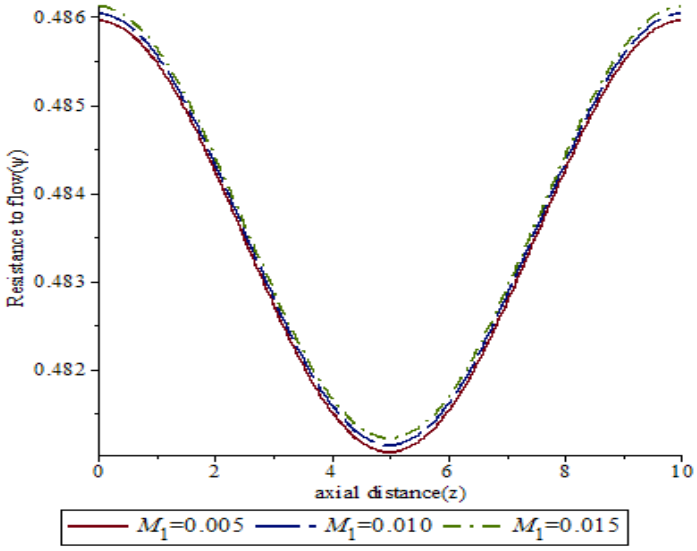

Figure 13a: Variation of Resistance to Unsteady Blood Flow Model with constant viscosity for various values of the Magnetic Field Parameter in the entire stenotic region along the axial direction.

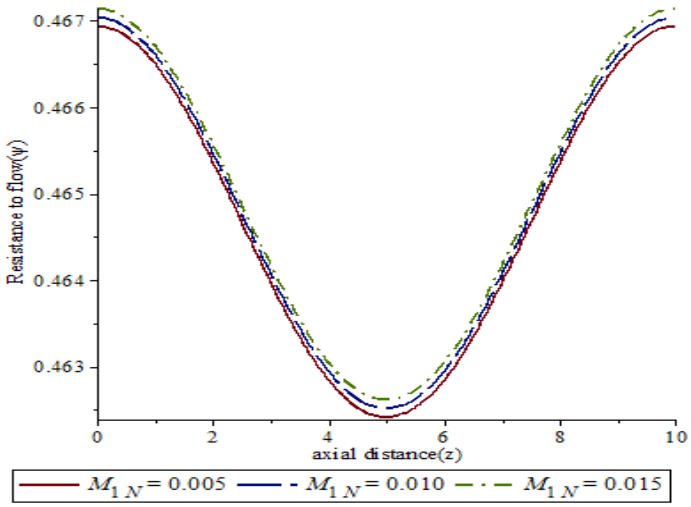

Figure 13b: Variation of Resistance to Unsteady Blood Flow Model with variable viscosity for various values of the Magnetic Field Parameter in the entire stenotic region along the axial direction.

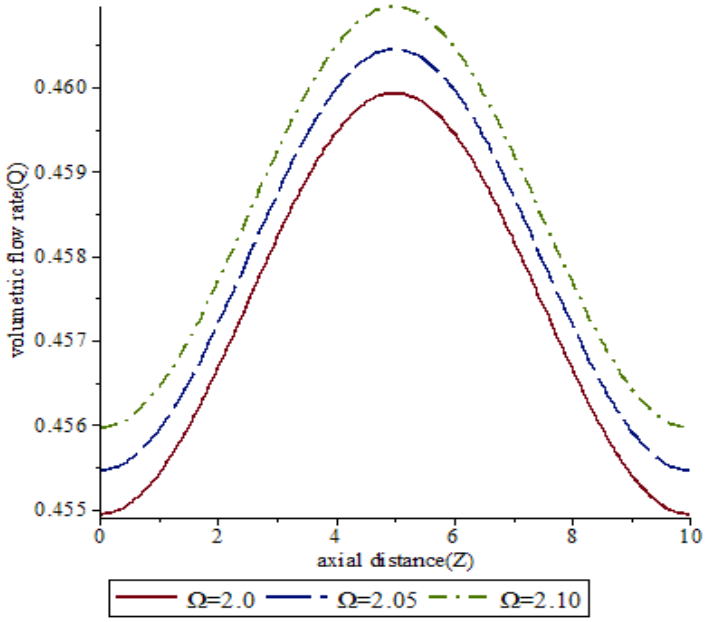

Figure 14a: Variation of Volumetric Flow Rate of Unsteady Blood Flow Model with constant viscosity for various values of the Shear thinning in the entire stenotic region along the axial direction.

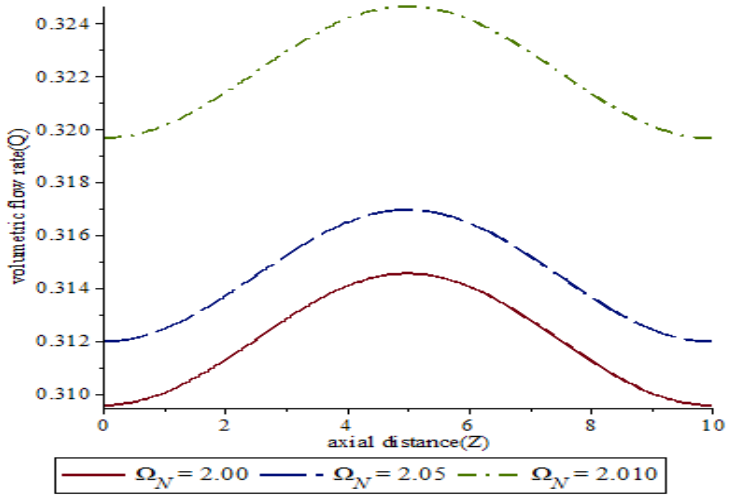

Figure 14b: Variation of Volumetric Flow Rate of Unsteady Blood Flow Model with variable viscosity for various values of the Shear thinning in the entire stenotic region along the axial direction.

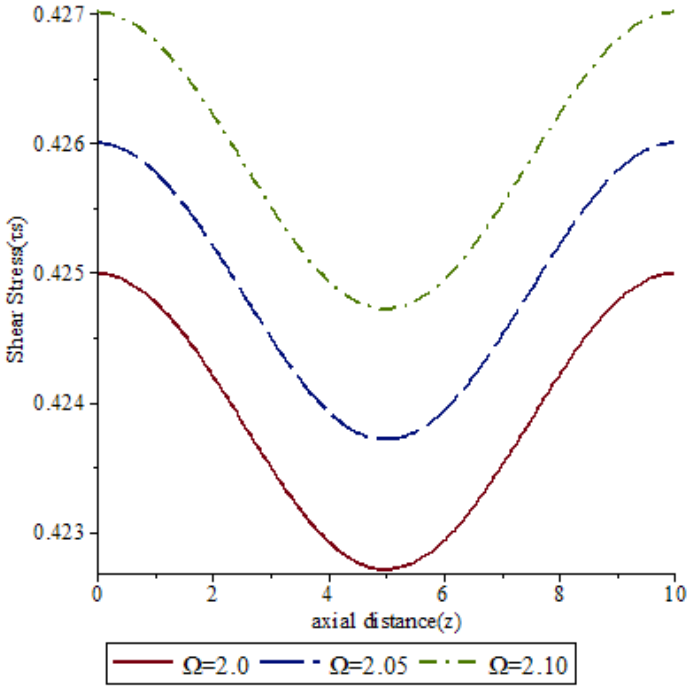

Figure 15a: Variation of Wall Shear Stress of Unsteady Blood Flow Model with constant viscosity for various values of the Shear Thinning in the entire stenotic region along the axial direction.

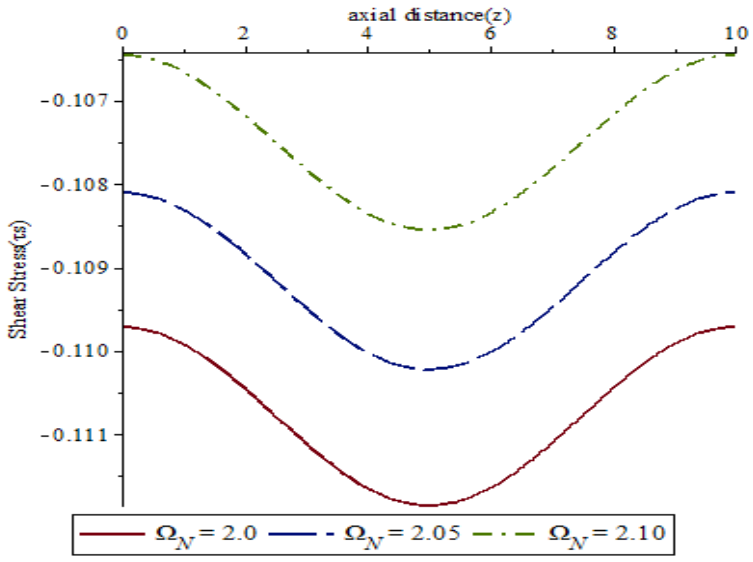

Figure 15b: Variation of Wall Shear Stress of Unsteady Blood Flow Model with variable viscosity for various values of the Shear Thinning in the entire stenotic region along the axial direction.

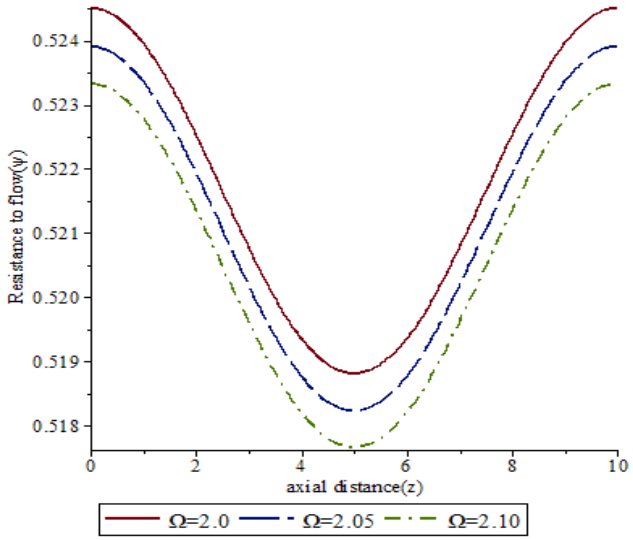

Figure 16a: Variation of Resistance to Unsteady Blood Flow Model with constant viscosity for various values of the Shear Thinning in the entire stenotic region along the axial direction.

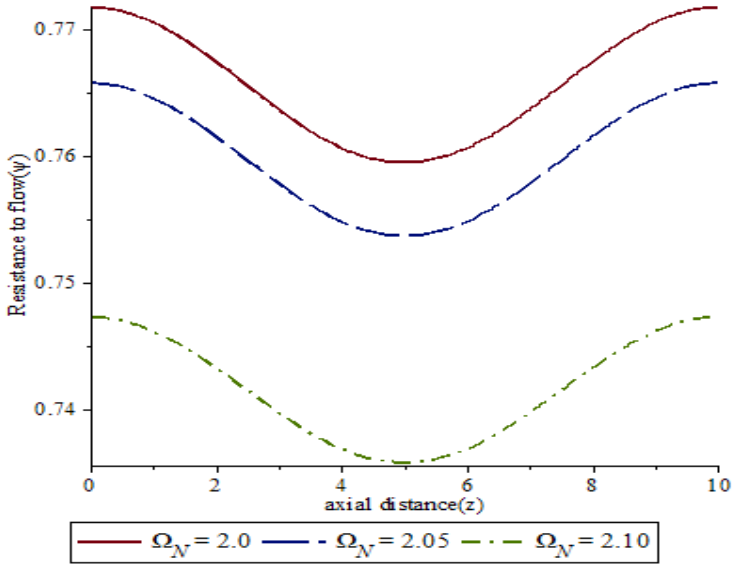

Figure 16b: Variation of Resistance to Unsteady Blood Flow Model with variable viscosity for various values of the Shear Thinning in the entire stenotic region along the axial direction.

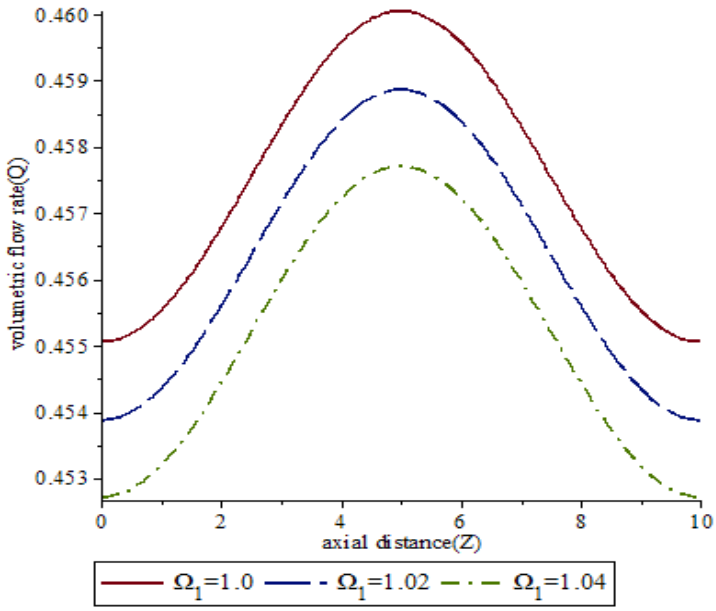

Figure 17a: Variation of Volumetric Flow Rate of Unsteady Blood Flow Model with constant viscosity for various values of the Shear Thickening in the entire stenotic region along the axial direction.

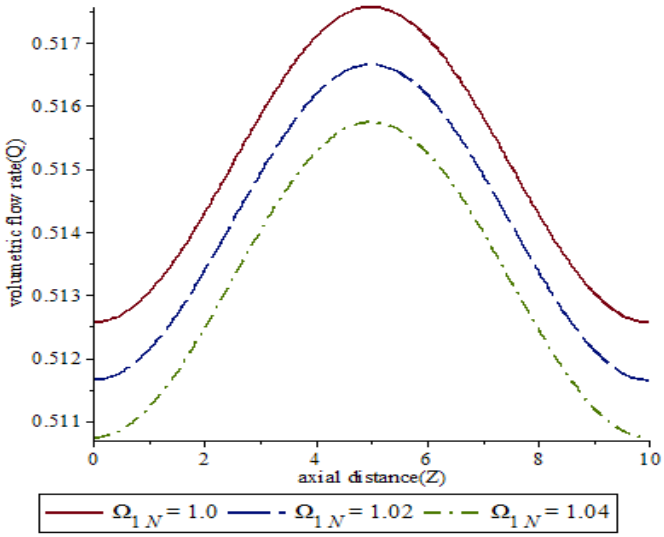

Figure 17b: Variation of Volumetric Flow Rate of Unsteady Blood Flow Model with variable viscosity for various values of the Shear Thickening in the entire stenotic region along the axial direction.

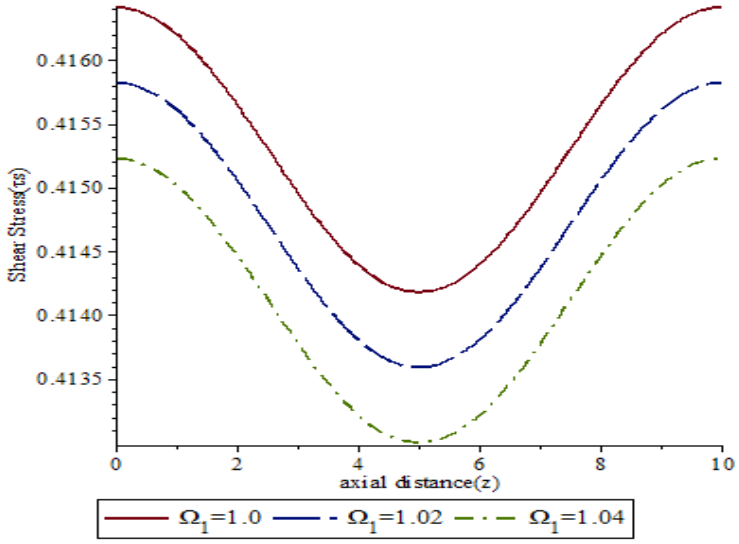

Figure 18a: Variation of Wall Shear Stress of Unsteady Blood Flow Model with constant viscosity for various values of the Shear Thickening in the entire stenotic region along the axial direction.

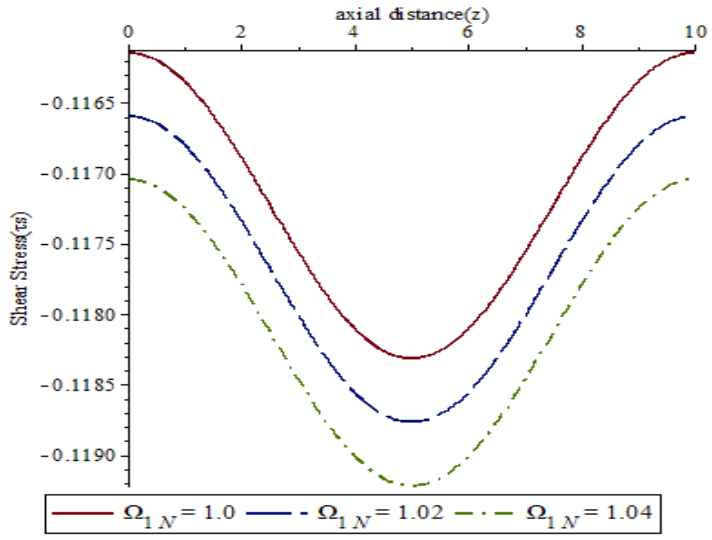

Figure 18b: Variation of Wall Shear Stress of Unsteady Blood Flow Model with variable viscosity for various values of the Shear Thickening in the entire stenotic region along the axial direction.

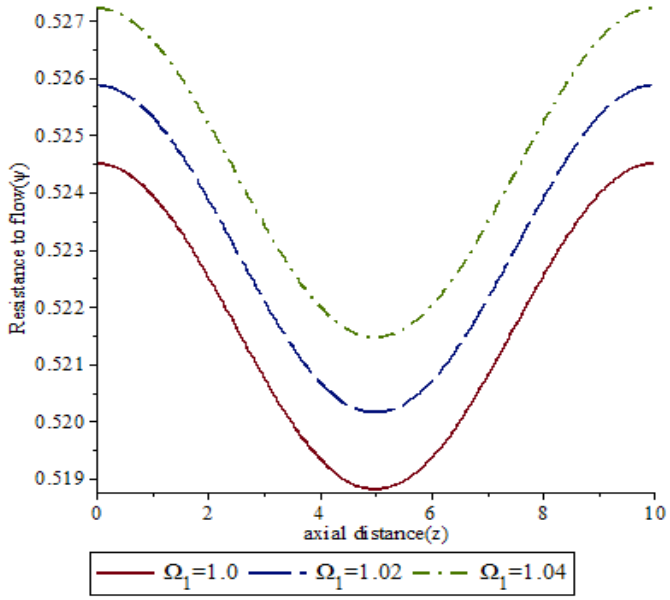

Figure 19a: Variation of Resistance to Unsteady Blood Flow Model with constant viscosity for various values of the Shear Thickening in the entire stenotic region along the axial direction.

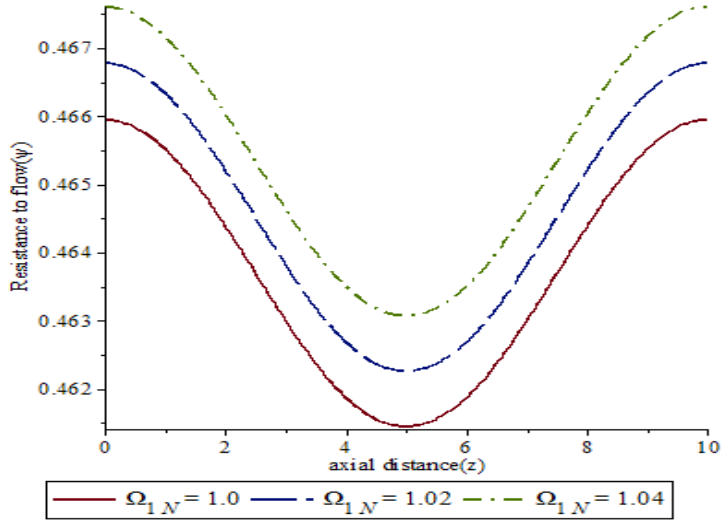

Figure 19b: Variation of Resistance to Unsteady Blood Flow Model with variable viscosity for various values of the Shear Thickening in the entire stenotic region along the axial direction.

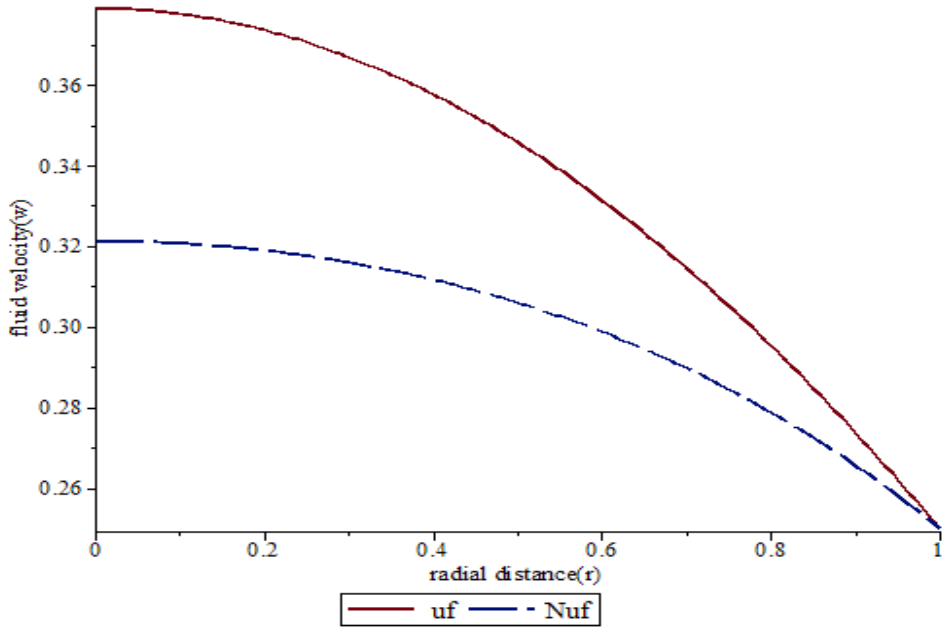

Figure20: Comparison of the Velocity Profile of Unsteady Blood Flow Models with Constant Viscosity and variable viscosity in the Radial Direction.

RESULTS AND DISCUSSION

In this study, numerical results have been made available to explore the effects of shear thinning, shear thickening, slip velocity and magnetic field parameter on the flow velocity, flow rate, shear stress and flow resistance. The presents mathematical problems are difficult to handle but computation and graphical representations with maple software make it easier. it was reveals that increases in slip velocity and shear thinning significantly lead to an increases in flow velocity, flow rate and shear stress but decrease the resistance to fluid flow for both flow model with constant viscosity and variable viscosity and these are shown in figures 4a, 4b, 8a, 8b, 9a, 9b, 10a,10b, 5a, 5b, 14a, 14b, 15a, 15b, 16a and 16b respectively. Increases in magnetic field parameter and shear thickening lead to deceases in flow velocity, flow rate, and shear stress but increase the resistances to fluid flow for the flow model with constant viscosity and variable viscosity and these are shown in figures 3a, 3b, 11a, 11b, 12a, 12b, 13a,13b, 6a, 6b, 17a, 17b, 18a, 18b, 19a and 19b respectively. Pressure gradient and Reynold number remarkably increases with flow velocity as shown in figures 2a, 2b, 7a and 7b respectively. Finally, the flow velocity of unsteady blood flow model with constant viscosity is higher than that with variable viscosity as indicated in figure 20.

Conclusion

A theoretical study of unsteady blood flow with constant and variable viscosities through a stenosed artery using a third grade fluid model has been carried out. In this study slip velocity and externally magnetic field are taken into consideration. The problems are solved using Galerkin weighted residual and forth order Runge-Kutta methods. The main findings of the present study may be listed as follows:

(i) The flow velocity, flow rate and shear stress decreases while flow resistance decreases with the increases of magnetic field strength and shear thickening for the blood flow models with constant and variable viscosities.
(ii) The flow velocity, flow rate and shear stress increases while flow resistance decreases with the increases of slip velocity and shear thinning for the blood flow models with constant and variable viscosities.
(iii) The effects of shear thinning, slip velocity, magnetic field and pressure gradient on the flow velocity are more pronounce and remarkable for the unsteady blood flow model with variable viscosity when compare to unsteady blood flow model with constant viscosity.
(iv) Finally, with fixed values of all the parameters, the velocity profile of the unsteady blood flow model with constant viscosity is higher than that with variable viscosity.

The research analysis incorporating slip velocity in the constricted artery can help to reduce blood viscosity because high blood viscosity is a risk factor in the cardiovascular disorder. Also, incorporating externally applied magnetic field will be useful for the reduction of blood flow during surgery and magnetic resonance imaging (MRI).

REFERENCE

1. Jimoh, A, Okedayo, G.T, and Aboiyar, T. (2018). Effects of Magnetic Field Slip Velocity on third Grade Blood Flow and Heat Transfer through a Stenosed Artery. *Mathematical Theory and Modelling. Vol. 8, NO. 8, Pp. 9-40.*

2. Jimoh, A, Okedayo, G.T, and Ikpakyegh, L. N. (2019). Computational Analysis of Unsteady Flow of Blood and Heat Transfer throug a Stenosed Artery in a third Grade Fluid Model with Slip Conditions. *International OF Applied Mathematics and Statistical Sciences. Vol. 8, Issue 5, Pp. 11-36.*

3. Aiman, A. and Bourhan, T. (2016). Simulation of MHD in Stenosed Arteries in Diabetic or Anemic model. *Computational and Mathematical Method in Medicine. 20: 1-13.*

4. Arun, K. M. (2016). Multiple Stenotic Effect of Blood Flow Characteristic in the Presence of Slip Velocity. *American Journal of Applied Mathematics and Statistics*, 4(6): 194-198.

5. Akbari, N., Ganji, D. D., Gholinia, M. and Gholinia, S. (2017). Computer Simulation of Blood Flow with Nano Particle in a Magnetic Field as a Third Grade Non-Newtonian through porous Vessel. *Innovative Energy and Research*, 6: 1-7.

6. Amit, B. and Shrivaster, C. (2014). Analysis of MHD Flow of Blood through a Multiple Stenosed Artery in the Presence of Slip Velocity. *International Journal of Innovative Research in Advanced Engineering*. 1(10): 3-15.

7. Tanwar, V. K. and Varshney, N. K. (2014). Pulsatile Flow of Blood through a Stenosed Artery body acceleration. *Uitra Scientist. Vol. 26, No 1B, Pp. 15-28.*

8. Ellahi, R., Rahman,. S. U. and Nadeem, S. (2014). Blood Flow of Jeffrey Fluid in Catherised Tapered Artery with the Suspension of Nanoparticles.
International Physics Letters A, 378(40), 2973-2980.

9. Hatami, M., Hatami, J. and Ganji, D. D. (2014). Computer Simulation of MHD Blood Conveying Gold Nanoparticles as a Third Grade Non-Newtonian Nano Fluid in a Hollow Porous Vessel. *Computer Method and Programs in Bio-Medicine,*133: 632-641.

10. Haleh, A., Mohsen, I. and Meadeh, S. (2014). Non-Newtonian Blood Flow in a Stenosed Artery with Porous Walls in the Presence of Magnetic Field Effect. *International Journal of Technology Enhancement and Emerging Engineering Research*, 12(8): 69-75.

11. Aziz, A. (2012). MHD Non-Newtonian Flow of Third Grade Fluid in a Porous Half Space with Plate Suction: An Analytical Approach. *Applied Mathematics and computation*, 218: 10443-10453.

12. Ikbal, M. A, Chakravarty, S., Wong, K. K. and Mandal, P. K. (2009). Unsteady Response of Non-Newtonian Blood Flow through a Stenosed Artery in Magnetic Field, *Journal Computational and Applied Mathematics*, 230(1): 243-259.

13. Misra, J. C. and Shit, G. C. (2007). Role of Slip Velocity in Blood Flow through Stenosed Arteries: A Non-Newtonian Model. *Journal of Mechanical in Medicine and Biology*, 7: 337-353.

14. Verma, N. K. and Parihar, R. S. (2010). Mathematical Model of Blood Flow through a Tapered Artery and Hematocrit. *Journal of Mathematics and Computer,1,30-36.*

15. Sanjeev, K and Chandraahekhar, D. (2015). Hematocrit Effect of the Axisymmetric Blood Flow through an artery with Stenosed Arteries. *International Journal of Mathematics Trends and Technology, 4, 91-96.*
16. Jimoh, A., Okedayo, G. T. and Aboiyar, T. (2013). Hematocrit and Slip Velocity Influence on Third Grade Blood Flow and Heat transfer through a Stenosed Artery. *Journal of Applied Mathematics and Physics, 7, 638-663.*
17. Mohammed, A. A. (2011). Analytical Solution for MHD Unsteady Flow of a Third Grade Fluid with Constant Viscosity. M.Sc. Thesis, Department of Mathematics, university of Baghdad. Pp. 1-104.
18. Jimoh, A. (2020). A Third Grade Fluid Model on the Influence of Hematocrit and Slip velocity on Blood Flow and Heat Transfer though a Stenosed Artery. Ph.D Thesis, Federal University of Agriculture, Makurdi, Benue State, Nigeria.
19. Young, D. F. (1979). Effect of Time Dependent Stenosis on Flow through a Tube. *Journal of Engineering*, 90: 248-254.
20. Biswas, D. (2000). Blood Flow Model: *A Comparative Study*. New Delhi:Mittal Publication. P. 15.

Nomenclatures

w - Fluid velocity
$\bar{w}$ - Dimensionless fluid velocity
t - Time component
$\bar{t}$ - Dimensionless time component
r - Radial distance
y - Dimensionless radial distance
z - Axial distance
w_s - Slip velocity
V_{01} - Dimensionless slip velocity for the unsteady blood flow with constant viscosity
V_{01N} - Dimensionless slip velocity for the unsteady blood flow with variable viscosity
R_0 - Radius of the normal artery
β_0 - Magnetic Field Strength
R(z) - Radius of the artery in a stenotic region
τ_s - Wall Shear Stress
ψ - Resistance to flow
$\mathcal{C}$ - Maximum height of the stenosis

Q - Volumetric flow rate
L - Length of the stenosis
W = Fluid velocity
G_1-Pressure gradient for the unsteady flow with constant viscosity
G_{1N}-Pressure gradient for the unsteady flow with variable viscosity
M_1-Magnetic field parameter for the unsteady flow with constant viscosity
M_{1N}-Magnetic field parameter for the unsteady flow with variable viscosity
Ω -Shear thinning for the unsteady flow with constant viscosity
Ω_N-Shear thinning for the unsteady flow with variable viscosity
Ω_1-Shear thickening for the unsteady flow with constant viscosity
Ω_{1N}-Shear thickening for the unsteady flow with variable viscosity
RE_1—Reynold number for the unsteady flow with constant viscosity
RE_{1N}—Reynold number for the unsteady flow with variable viscosity